PAPER

A hybrid method combining the surface integral equation method and ray tracing for the numerical simulation of high frequency diffraction involved in ultrasonic NDT

IOP Conf. Series: Journal of Physics: Conf. Series **1017** (2018) 012007 doi:10.1088/1742-6596/1017/1/012007

A hybrid method combining the surface integral equation method and ray tracing for the numerical simulation of high frequency diffraction involved in ultrasonic NDT

M Bonnet[1], F Collino[2], E Demaldent[3], A Imperiale[3], L Pesudo[1,3]

[1] POEMS, CNRS-INRIA-ENSTA UMR 7231,
ENSTA Paristech, 828 boulevard des Marchaux, 91120 Palaiseau, France
[2] 39 rue de Montreuil 75011 Paris
[3] CEA, institut LIST, Centre de Saclay, Bat 565 Digiteo Labs, 91191 Gif-sur-Yvette, France

E-mail: laure.pesudo@ensta-paristech.fr

Abstract. Ultrasonic Non-Destructive Testing (US NDT) has become widely used in various fields of applications to probe media. Exploiting the surface measurements of the ultrasonic incident waves echoes after their propagation through the medium, it allows to detect potential defects (cracks and inhomogeneities) and characterize the medium. The understanding and interpretation of those experimental measurements is performed with the help of numerical modeling and simulations. However, classical numerical methods can become computationally very expensive for the simulation of wave propagation in the high frequency regime. On the other hand, asymptotic techniques are better suited to model high frequency scattering over large distances but nevertheless do not allow accurate simulation of complex diffraction phenomena. Thus, neither numerical nor asymptotic methods can individually solve high frequency diffraction problems in large media, as those involved in UNDT controls, both quickly and accurately, but their advantages and limitations are complementary. Here we propose a hybrid strategy coupling the surface integral equation method and the ray tracing method to simulate high frequency diffraction under speed and accuracy constraints. This strategy is general and applicable to simulate diffraction phenomena in acoustic or elastodynamic media. We provide its implementation and investigate its performances for the 2D acoustic diffraction problem. The main features of this hybrid method are described and results of 2D computational experiments discussed.

1. Motivations

Ultrasonic Non-Destructive Testing (US NDT) aims at probing continuous media by propagating high frequency waves. During an Ultrasonic Non-Destructive test, a wave is generated outside the material and propagates through the medium, bouncing back against interfaces and diffracting from edges or small defects (inclusions, cracks...). Its propagation response is detected by receivers placed at the surface of the medium and analyzed to obtain useful information on the structure and integrity of the probed material. Numerical simulation has become an important tool to understand and interpret those measurements, allowing to detect and characterize surface breaking or internal defects. It has also become of great interest to help

designing and optimizing inspection protocols. In a nutshell, the development of high frequency cost-effective simulation tools well-adapted for industrial use progressively made it possible for US NDT to be assisted by numerical simulations. The computational strategy of these tools is of major importance and should both allow fast computations and good approximations of complex diffraction phenomena.

In the second half of the 20th century, asymptotic methods were specifically designed to deal with wave scattering problems at high frequency regimes. They allow fast non-dispersive computations of the wave scattering over large scales and give quantitative predictions of its diffraction in a large range of configurations. However, they fail in predicting accurately the complex phenomena occuring at the wavelength scale, e.g. diffraction by small defects, or interactions between multiple defects or a defect and an interface. Besides, they lack generality as those methods do not take into account the physical phenomena arising at the different scales, such as scattering over large distances, specular reflection, transmission across an interface, diffraction by a corner. All those phenomena require additional scale-specific asymptotic modeling.

On the other hand, classical numerical methods, such as the finite difference (FD) method, the finite element method (FEM) or the boundary element method (BEM) allow to compute a very accurate numerical approximation of the complex multiscale diffraction problem involved in the NDT configurations and modeled by a partial differential equation. They nevertheless entail excessive time and memory costs at high frequencies.

Consequently, neither family of methods can individually solve high frequency diffraction problems in large media both fast and accurately. However, their combination into a hybrid strategy leads to a good compromise between accuracy and computational cost for such critical configurations. In this work we propose a new hybrid strategy that combines the surface integral equation method [3] and the ray tracing method [6]. This hybrid method relies on a two-scale model of a diffracting defect, which allows to separate the treatement of the propagation and diffraction phenomena. The propagation effects are computed using the ray tracing asymptotic method, a Lagrangian formulation of geometrical optics based on a WKB ansatz for the solution of the wave equation [6]. The diffraction phenomena are predicted accurately by the BEM.

This paper is devoted to the formulation and computational demonstration of our multi-scale hybrid strategy. Section 2 introduces the model problem, for which the hybrid solution strategy is formulated in section 3. Then an accelerated version of this strategy is outlined in section 4 in view of NDT applications. Finally, numerical results that demonstrate implementation of the hybrid method for a 2D acoustic model problem are presented in section 5.

2. Model problem

We consider a model problem of 2D time-harmonic acoustic scattering of an incident wave u^{i}, propagating in a large bounded medium Ω, by a sound-soft diffracting obstacle $\Omega_0 \subset \Omega$ with the boundary Γ, as illustrated in Figure 1. The model problem is described by the Dirichlet problem for the 2D Helmholtz equation,

$$\begin{cases} \Delta u + k^2 u = 0, & \text{in } \Omega, \\ u = -u^{\mathrm{i}}, & \text{on } \Gamma, \end{cases} \tag{1}$$

where u is the unknown diffracted field. The incident field u^{i} is created by an excitation in the defect-free domain Ω. Additionally to (1), u satisfies some (unspecified) homogeneous boundary conditions on $\partial\Omega$, of the same type as the ones verified by u^{i}. We denote by x_s and x_r respectively the positions of the source S and the observation point or receiver R, and $k = \frac{2\pi f}{c}$ is the wave number associated to the incident wave emission frequency f and the medium velocity c. Some important geometrical hypotheses must now be added to describe the setting of the model

IOP Conf. Series: Journal of Physics: Conf. Series **1017** (2018) 012007 doi:10.1088/1742-6596/1017/1/012007

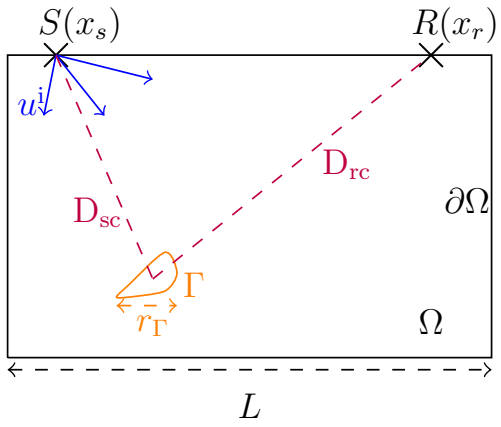

Figure 1: Diffraction configuration for the model problem.

problem (figure 1). First, the obstacle Ω_0 is supposed to be impenetrable and diffracting. Its characteristic size r_Γ is defined as

$$r_\Gamma = 2\max_{y\in\Gamma}(|y - y_c|),$$

as the diameter of the smallest disk containing Ω_0 and centered at the defect centroid y_c. It is assumed to satisfy $r_\Gamma = O(\lambda)$. Second, the propagating medium Ω is supposed to be large with respect to the wavelength ($L \gg \lambda$), isotropic and homogeneous. We assume the velocity of the wave in Ω $c = 1$. Third, both the source and the receiver are supposed to be located far enough from the defect to allow an accurate approximation of the incident and the diffracted fields by rays impinging on, or emanating from, the defect. Setting $\mathrm{D_{sc}} = |x_s - y_c|$ and $\mathrm{D_{rc}} = |x_r - y_c|$, this hypothesis requires satisfying $k\mathrm{D_{sc}} \gg 1$ and $k\mathrm{D_{rc}} \gg 1$. Finally, we suppose the defect to be located far enough from the medium boundary $\partial\Omega$ so that the interactions of the incident and diffracted fields with $\partial\Omega$ can be viewed and computed as reflections in the sense of geometrical optics. Under this framework, the contributions of the reflections of the incident and diffracted rays on $\partial\Omega$ are neglected on the defect. We approximate the incident field at each point of Γ $(x_j)_{j\in[1:N_d]}$ as a ray characterized by its amplitude A_j^s and phase ϕ_j^s:

$$u_{\mathrm{inc}}(x_j) = A_j^s e^{i\omega\phi_j^s}, \tag{2}$$

and the diffracted field at x_r as a sum of all the rays $(B_j^r, \phi_j^r)_{j\in[1:N_d]}$, emitted towards x_r from points of Γ:

$$u(x_r) = \sum_{j=1}^{N_d} B_j^r e^{i\omega\phi_j^r}. \tag{3}$$

For more accuracy during a Non-Destructive inspection, the sources and receivers are in practice sequentially moved around the probed medium. Consequently, realistic NDT configurations demand to compute the diffracted field at multiple positions of the receiver for multiple source positions. However, at ultrasonic regimes, an accurate representation of those fields requires a spatial discretization of Γ whose meshsize scales with $1/f$, making representations (2) and (3) computationally very expensive. The hybrid strategy proposed in this work relies on a two-scale model of the obstacle Ω_0 that allows to approximate the incident and diffracted field on Γ using a small number of rays.

IOP Conf. Series: Journal of Physics: Conf. Series **1017** (2018) 012007 doi:10.1088/1742-6596/1017/1/012007

3. The two-scale solution approach

The high frequency diffraction model problem is a multi-scale problem. We can identify at least two scales with respect to the wavelength on which the physics of the wave propagation is different: the propagating medium scale $L = O(100\lambda)$, corresponding to the high frequency wave propagation phenomena, and the obstacle scale, $O(\lambda)$, at which the interaction of the incident wave with the obstacle Γ generates diffraction phenomena. The hybrid strategy proposes a two-scale model of the obstacle Γ which allows to dissociate computations of propagation and diffraction phenomena. The solution of the model problem by the hybrid strategy is thus decomposed into three independent stages:

- the propagation of the incident wave u^{i} from the source S to the obstacle,
- the diffraction by the obstacle,
- the propagation of the scattered field from the obstacle to the receiver R.

Each stage is solved separately by a scale-specific method. The high frequency propagation phenomena being well modeled by Geometrical Optics laws, the two propagation problems are solved by the asymptotic ray tracing method. For those stages, set on the propagation (large) scale, the obstacle, is modeled by means of a small number P of well-chosen points close to Γ which allow to approximate the incident and diffracted fields on Γ as the plane wave approximations of the rays received at, or emitted by, those points. Diffraction coefficients, which carry information about the obstacle geometry and characteristics, are associated to these points, called centers and denoted by $(y_c^p)_{p\in[1:P]}$. Solving the propagation problems thus comes down to shooting rays from the source to each y_c^p and from the latter to the observation point. We hence expect a fast computation of the propagation phenomena. The validity of this model will be discussed in more detail in sections 3.1 and 3.2.

The diffraction phenomena are computed by the integral equation method in order to accurately describe the physics of the scattering problem at the obstacle scale. For this stage, the obstacle is described by its exact geometry. Still, in the model problem setting, the interactions of diffracted waves with the medium boundary $\partial\Omega$ are modeled as high frequency propagation phenomena, consequently the scattering by Γ is computed as the outgoing solution of the scattering problem in an unbounded medium:

$$\begin{cases} \Delta u + k^2 u = 0, & \text{in } \mathbb{R}^2 \setminus \bar{\Omega}_0, \\ u = -u^{\mathrm{i}}, & \text{on } \Gamma, \\ \lim\limits_{|x|\to\infty} \sqrt{|x|}\left(\dfrac{\partial u}{\partial |x|} - ik\,u\right) = 0. \end{cases} \tag{4}$$

Finally, the results of the three stages are recombined to evaluate the diffracted field at the receiver.

Before getting into more details on the description of the two-scale solution approach outlined above, we briefly describe the methods chosen to compute the propagation and diffraction stages.

The ray tracing method. The ray tracing method is a Lagrangian formulation of geometrical optics based on the representation of high frequency waves v by a WKB ansatz [6] having the form

$$v(x) = A(x)e^{i\omega\phi(x)}.$$

This ansatz allows to characterize the leading-order contribution to the highly oscillatory field u as $f^{-1} \to 0$ by two frequency independent functions A and ϕ, respectively the amplitude and

phase of the ray, which evolve on a much coarser grid than v. They are respectively evaluated by numerical integration of the eikonal and transport equations

$$\begin{cases} |\nabla\phi(x)| = 1, \\ 2\nabla\phi(x)\cdot\nabla A(x) + A(x)\Delta\phi(x) = 0, \end{cases} \tag{5}$$

along specific trajectories called rays which are the characteristics of the eikonal equation. In particular, the rays propagating in a homogeneous medium are straight lines.

In the hybrid solution procedure, the computation of the incident and diffracted wave fields will respectively consist in evaluating the amplitudes and phases $(A_p^s(y_c^p;x_s),\phi_p^s(y_c^p;x_s))$ of the rays propagating from the source x_s to each center y_c^p knowing the incident field value at the source, and the amplitude and phase $(A_p^r(x_r;y_c^p),\phi_p^r(x_r;y_c^p))$ of the unique ray emitted by each center, with unit amplitude and zero phase, to the observation point x_r.

The integral equation method. The integral equation method seeks the radiating solution of a well posed propagation problem in the form of a surface integral representation [2, 3]. Here, to solve the diffraction problem described by (4), we consider the equivalent surface problem described by the indirect Brackhage-Werner surface integral equation

$$\frac{\Psi(x)}{2} + \int_\Gamma \left(\frac{\partial G}{\partial\nu(y)} - \mathrm{i}kG\right)(x,y)\Psi(y)ds(y) = -u^{\mathrm{i}}(x),\ \forall x\in\Gamma, \tag{6}$$

which is well-posed for any frequency [3]. Here G denotes the fundamental solution of the 2D Helmholtz equation in an infinite medium, i.e. $G(x,y) = \frac{\mathrm{i}}{4}H_0^1(k|x-y|)$. This integral equation is then numerically solved by the boundary element method to obtain the surface density Ψ on Γ. Applying the integral representation formula

$$u(x_r) = \int_\Gamma \left(\frac{\partial G}{\partial\nu(y)} - \mathrm{i}kG\right)(x,y)\Psi(y)ds(y), \tag{7}$$

one then computes the outgoing solution of the diffraction problem at any point $x_r\in\Omega$.

The diffraction and propagation solution methods are independent, and rely on distinct modeling of the diffracting obstacle. To recombine their results, the hybrid strategy exploits the model problem hypotheses. If the obstacle Γ is in the far field zone of the source and receiver, depending on its size, the diffracted field at x_r can be rewritten either as a ray or as a superposition of rays with an amplitude weighted by a diffraction coefficient. This approximation and its validity conditions are now described.

3.1. The barycentric method

When the diffracting obstacle Ω_0 is small enough with respect to the wavelength and situated in the far field zone of the source and the receiver, i.e. when it fulfills the conditions

$$\begin{cases} kD_{\mathrm{sc}} \gg 1, \quad \text{and} \quad kD_{\mathrm{rc}} \gg 1 \\ kr_\Gamma = O(1), \\ \dfrac{kr_\Gamma^2}{8D_{\mathrm{sc}}} \ll 1 \quad \text{and} \quad \dfrac{kr_\Gamma^2}{8D_{\mathrm{rc}}} \ll 1, \end{cases} \tag{8}$$

the defect can be modeled at the propagation scale as the neighbourhood of a single point, its centroid y_c. This point receives a single ray from the source $(A^s(y_c;x_s),\phi^s(y_c;x_s))$ and emits a single diffracted ray $(A^r(x_r;y_c),\phi^r(x_r;y_c))$ to the receiver.

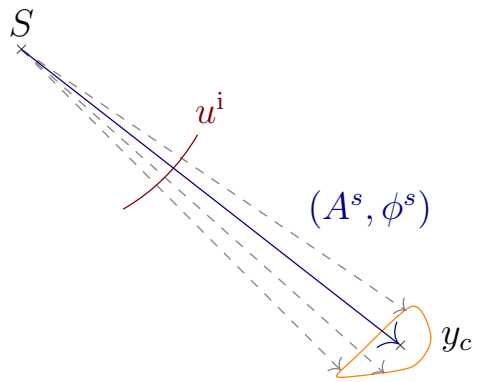

Figure 2: Ray approximation u^{i}.

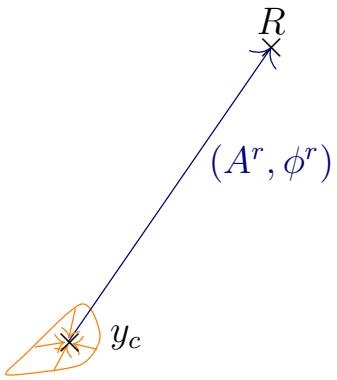

Figure 3: Ray approximation of diffracted field.

Besides, the far field hypotheses allow to link the ray approximations of the incident and diffracted fields to the solution of the diffraction problem. First, to solve the diffraction problem the incident field must be evaluated on each point of Γ from the incident ray amplitude and phase. Under conditions (8), the incident field is approximated on Γ as the linearisation $\tilde{u}^{\mathrm{i}}$ of the incident ray $(A^s(y_c; x_s), \phi^s(y_c; x_s))$:

$$\forall y \in \Gamma, \quad \tilde{u}^{\mathrm{i}}(y) := A^s(y_c; x_s)\, e^{i\omega\phi^s(y_c;x_s)}\, e^{i\omega\hat{s}(y-y_c)}, \tag{9}$$

where the unit vector $\hat{s} = \frac{y_c - x_s}{|y_c - x_s|}$ denotes the direction of propagation of the incident ray. Second, to match the hybrid strategy propagation model, the diffracted field obtained numerically by the integral representation formula (7) has to be converted into a ray. Under conditions (8), (7) can be approximated by its far field expansion:

$$u(x_r) = \frac{e^{ik|x_r - y_c|}}{\sqrt{|x_r - y_c|}}\, \mathcal{R}(\hat{r}, \hat{s})\, A^s(y_c; x_s)\, e^{i\omega\phi^s(y_c;x_s)} + o\left(\frac{1}{k\|x_r - y_c|}\right), \tag{10}$$

which can be interpreted as a ray propagating from the centroid y_c to the observation point x_r, its amplitude being weighted by the complex amplitude of the incident ray at y_c and the coefficient $\mathcal{R}$ given by

$$\mathcal{R}(\hat{r}, \hat{s}) := \sqrt{\frac{-ik}{8\pi}} \int_\Gamma e^{-ik\hat{r}\cdot(y-y_c)}\, (\nu(y)\cdot\hat{r} + 1)\, \Psi(y) ds(y), \tag{11}$$

defined as the far field amplitude of (7). Here Ψ is the exact solution of the surface integral problem (6) with $u^{\mathrm{i}}(y) = e^{ik\hat{s}\cdot(y-y_c)}$.

The coefficient $\mathcal{R}$ can be interpreted as the diffraction coefficient in the direction $\hat{r}$ of the obstacle Γ illuminated by an incident plane wave of unit amplitude and direction of propagation $\hat{s}$. It only depends on the incidence and observation directions, on the frequency and on the surface Γ. Equation (9) effectively converts the diffracted field into a ray since the amplitude $A(z) = 1/\sqrt{|z|}$ and phase $\phi(z) = |z|$ functions in the order 0 WKB expansion-like function $v(|x_r - y_c|) = \frac{e^{i|x_r - y_c|\omega/c}}{\sqrt{|x_r - y_c|}}$ satisfy the eikonal and transport equations (5).

The framework of the barycentric method is efficient but may impose excessive restrictions on the obstacle size, as shown by numerical results presented in section 5. In particular the method accuracy deteriorates as the obstacle diameter increases, all other parameters being kept fixed. The hybrid strategy has thus been extended as follows to deal with bigger obstacles.

3.2. The polycentric method

This extension aims at computing the diffraction effects of a diffracting obstacle whose diameter is of order one or a few wavelengths, i.e. $r_\Gamma = O(\lambda)$. Because of its size, the obstacle is no longer in the far field zone of the source and the receiver, and will no longer be modeled as a single point at the propagation scale. The remedy consists in introducing a partition of unity of Γ, characterized by a distribution of points $y_c^p \in \Gamma$ called centers and smooth nonnegative partitioning functions $(\eta_p)_{1\leq p\leq P}$, defined on Γ and verifying

$$\sum_{p=1}^{P} \eta_p(x) = 1, \forall x \in \Gamma.$$

The supports Γ_p of the functions η_p define a covering of Γ, $\Gamma = \bigcup_{p=1}^{P} \Gamma_p$. For implementation purposes, we consider a diffracting disk and a uniform distribution of the centers y_c^p. We then define the subsets Γ_p as the intersection of Γ with the disk of center $y_c^p \in \Gamma$ and radius $r^p = |y_c^p - y_c^{p+1}|$ (with $y_c^{P+1} = y_c^1$)

$$\Gamma_p = \{y \in \Gamma \,|\, |y - y_c^p| < r^p\}\,.$$

The number P is chosen to guarantee that each subset is small enough to be in the far field

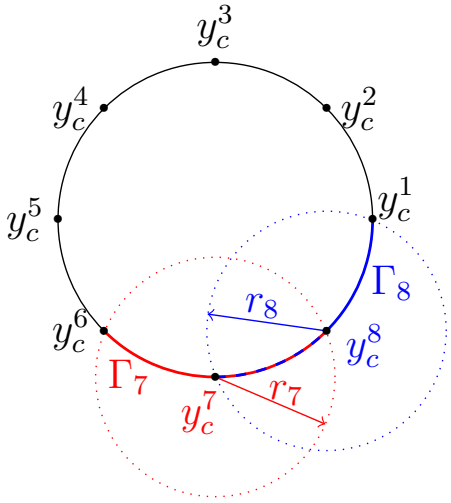

Figure 4: Covering of Γ.

zone of the source and receiver, i.e. satisfies

$$\begin{cases} kr_p = O(1), \\ \dfrac{kr_p^2}{2D_{\text{sc}}} \ll 1 \quad \text{and} \quad \dfrac{kr_p^2}{2D_{\text{rc}}} \ll 1, \end{cases} \qquad p \in [1:P]. \tag{12}$$

Under these hypotheses, the obstacle is modelled at the propagation scale as a set of P points y_c^p, each receiving a single ray propagated from the source in the direction $\hat{s}^p = \frac{y_c^p - x_s}{|y_c^p - x_s|}$ and emitting a single diffracted ray of unit amplitude and zero phase from y_c^q to the observation point x_r in the direction $\hat{r}^q = \frac{x_r - y_c^q}{|y_c^q - x_r|}$. The amplitudes and phases of those rays are computed

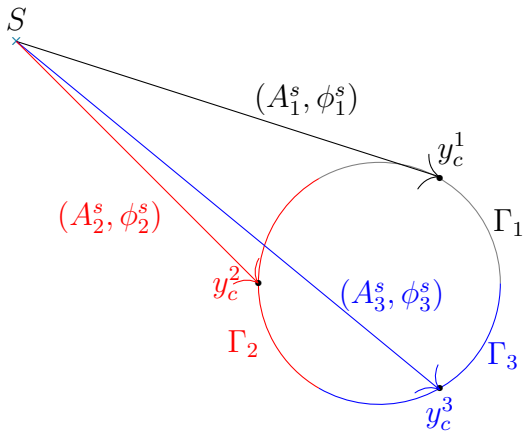

Figure 5: Ray propagation of the incident field.

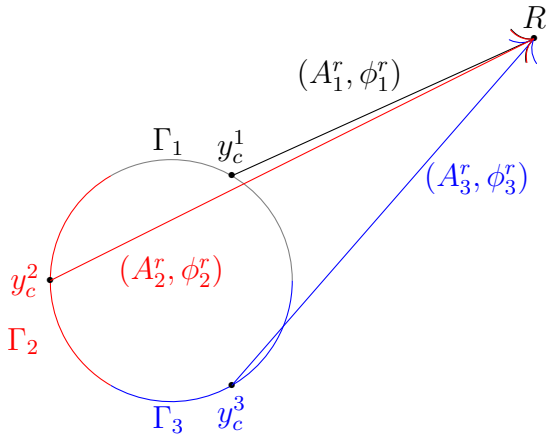

Figure 6: Ray propagation of the diffracted field.

by the ray tracing method.

As for the barycentric method, two approximations have to be introduced, one on the incident field and one on the diffracted field, to ease the recombination of the results obtained at the propagation and diffraction scales. First, to allow the solution of the diffraction problem by the integral equation method, the incident field u^{i} is approximated on each subset as the plane wave approximation $u^{\mathrm{i},p}$ of its corresponding incident ray $(A_p^s(y_c^p; x_s), \phi_p^s(y_c^p; x_s))$, i.e.:

$$\forall y \in \Gamma, \quad \tilde{u}^{\mathrm{i}}(y) = \sum_{p=1}^{P} \eta_p(y)\, \tilde{u}^{\mathrm{i},p}(y) = \sum_{p=1}^{P} \eta_p(y)\, A_p^s(y_c^p; x_s)\, e^{i\omega\phi_p^s(y_c^p;x_s)}\, e^{i\omega\hat{s}^p(y-y_c^p)}. \tag{13}$$

Second, subject to the conditions (12), the diffracted field at the receiver is converted into the superposition of P diffracted rays emitted from the centers y_c^p:

$$u(x_r) = \sum_{q=1}^{P} \frac{e^{ik|x_r - y_c^q|}}{\sqrt{|x_r - y_c^q|}} \sum_{p=1}^{P} \mathcal{R}_p^q(\hat{r}^q, \hat{s}_p)\, A_p^s(y_c^p; x_s)\, e^{i\omega\phi_p^s(y_c^p;x_s)}, \tag{14}$$

and weighted by the diffraction coefficient $\mathcal{R}_p^q$ of the qth partition when considering the contribution of the pth partition to the incident field approximation:

$$\mathcal{R}_p^q(\hat{r}^q, \hat{s}^p) = \sqrt{\frac{-ik}{8\pi}} \int_\Gamma \eta_q(y)\, e^{-ik\hat{r}^q\cdot(y-y_c^q)}\, (\nu(y)\cdot\hat{r}^q + 1)\, \Psi^p(y) ds(y), \tag{15}$$

where Ψ^p is the exact solution of the surface integral equation (6) with $u^{\mathrm{i}}(y) = e^{ik\hat{s}^p\cdot(y-y_c^p)}$.

The covering of Γ thus uncouples the role of each subset, both in terms of reception of the incident field and emission of the diffracted field allowing a muti-scale resolution. The accuracy of the evaluation of the diffracted field by this extension increases with the number of partitions (along with its computational cost).

4. Online-Offline acceleration

Considering the need for an efficient simulation of realistic NDT diffraction configurations, where multiple source and receiver positions are involved together with large numbers of

pairs of incident and diffraction directions, we additionally developed an acceleration of the hybrid strategy based on an online-offline procedure. This procedure aims at reducing the computational cost of the diffraction coefficient evaluation, which represents the most expensive operation in the hybrid solution procedure. Offline, the matrix of the diffraction coefficients is evaluated at predefined incident and diffraction directions, and its truncated low rank approximation computed by a SVD [8]. Online, the polynomial interpolation of the singular functions in the direction of interest is evaluated and used to compute an approximation of the diffraction coefficients in those directions. The acceleration was found in 2D numerical tests to be effective if the number of evaluation directions exceeds about 200, and is expected to perform even better under 3D conditions.

5. Numerical results

This section presents the numerical results of the implementation of the barycentric and polycentric versions of our hybrid strategy to a 2D acoustic problem. We consider a circular defect of characteristic size r_Γ, a source point S situated at 120λ from the defect centroid y_c and an annulus of receivers around Γ bounded by circles centered at y_c and of radius 5λ, 65λ, as depicted on Figure 7. The range of distances of the receivers to the centroid are representative of the typical distances between the probe and the controlled region in realistic NDT experiments. The numerical results presented here aim at showing that the hybrid strategy proposed allows a good accuracy in the whole range of relevant distances.

5.1. The barycentric solver

We begin by testing the performances of the barycentric method on the chosen configuration for a diffracting obstacle Γ of size $r_\Gamma = 0.3\lambda$. The barycentric method computes the diffracted field with good accuracy, as shown on the map of relative error of the diffracted field with respect to the reference solution obtained on the annulus of receivers (Figure 8) by the highly accurate Nystrom method. Besides, we notice that the relative error decreases quickly with the distance of y_c to the receiver, as shown in Table 1, where the angular maximum of the relative error, denoted by $\max_\theta(\text{er})$, is given for increasing observation distances $\mathrm{D_{rc}}$. The largest relative error reached at 5λ is 1.2%, indicating a resonably good precision of the barycentric method in the near field given the order of accuracy that the ray tracing method allows. If we now consider

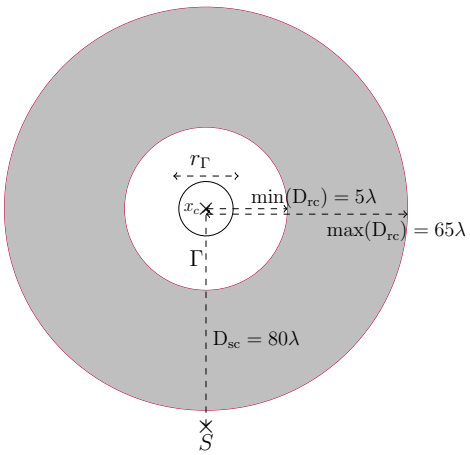

Figure 7: Numerical experiment configuration.

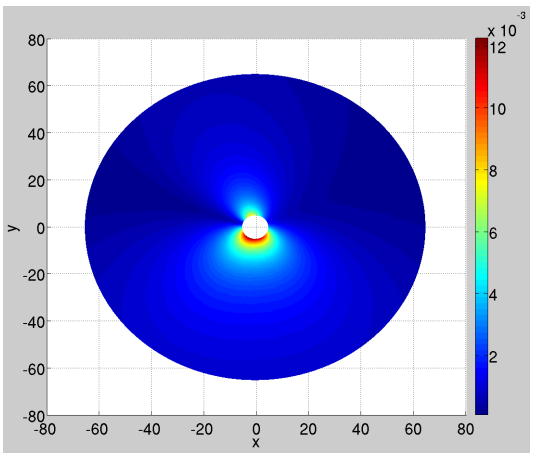

Figure 8: Map of relative error er of the diffracted field for a barycentric resolution, $r_\Gamma = 0.3\lambda$.

Table 1: Evolution of the relative error with respect to the distance to Γ, $r_\Gamma = 0.3\lambda$.

D_{rc}/λ	5	10	20	30	40	50	60	65
$\max_\theta(\text{er})$ $(\times 10^{-3})$	12.52	5.99	3.02	2.02	1.51	1.21	1.01	0.93

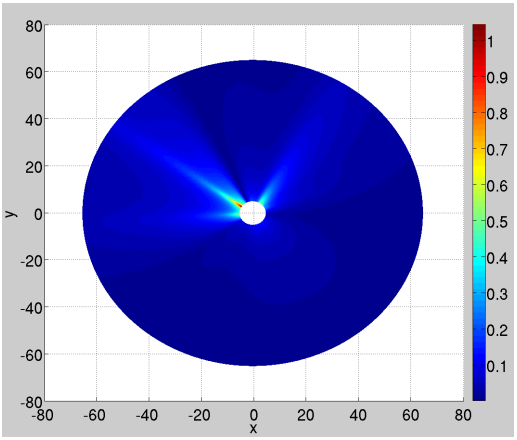

Figure 9: Map of relative error er of the diffracted field using the barycentric method, $r_\Gamma = 2\lambda$.

D_{rc}/λ	$\max_\theta(\text{er})$
5	1.045
10	0.536
20	0.278
30	0.181
40	0.136
50	0.109
60	0.084
65	0.084

Table 2: Evolution of the relative error with respect to the distance to Γ, $r_\Gamma = 2\lambda$.

a larger diffracting obstacle of size $r_\Gamma = 2\lambda$, in the same experimental setting, the barycentric method fails at giving such a good accuracy. Figure 9 displays the map of relative errors of the diffracted field computed by the barycentric method with respect to the reference solution and Table 2 provides values of the relative error.

5.2. The polycentric solver

In this section, we illustrate how the polycentric version of the hybrid strategy improves the accuracy of the computation of the diffraction effects by a disk of diameter $r_\Gamma = 2\lambda$. As expected, the accuracy of the evaluation of the diffracted field on the annulus of receivers is rapidly increased for a sufficient number of partitions. Figure 10 shows the map of relative error for the diffracted field computed using a covering of Γ by 16 subsets. It shows a maximum relative error at 5λ of 2.29%. This covering allows to reach maximum relative error of the same order as that of the ray tracing method. Besides, to show the evolution of the maximum of the relative error with respect to the number of subsets, we conducted several numerical experiments for subdivions of Γ involving 3 to 40 subsets. The evolution of the maximum of the relative error at 5λ from y_c with respect to the number of subsets is plotted on figure 11. We notice that the maximum relative error can be decreased to an asymptotic value of 1%.

6. Conclusion

A hybrid strategy combining the ray tracing method and the integral equation method was here proposed to allow a good high frequency approximation of the diffraction phenomena both in the far field and near field zones. The strategy principle was described on a simplified configuration, where the diffracting obstacle is supposed to be far from the boundaries of an homogeneous propagating medium. Nevertheless, the strategy is also applicable in the more relevant configuration of propagation in a large homogeneous medium containing multiple inhomogeneities. Besides, current work aims at extending the presented approach to cases where

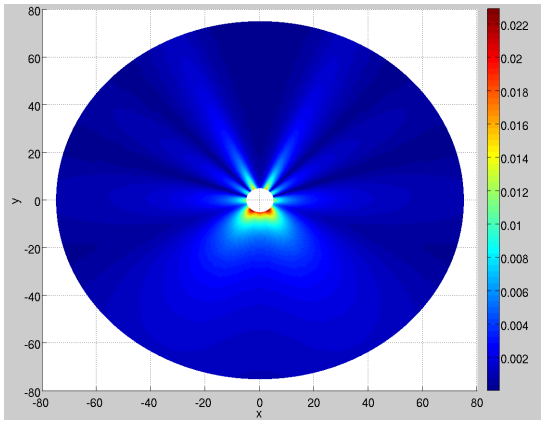

Figure 10: Map of relative error er of the diffracted field using the polycentric method, $r_\Gamma = 2\lambda$, $P = 16$.

D_{rc}	$\max_\theta(\text{er})$ $(\times 10^{-3})$
5	22.9
10	10.8
20	5.24
30	3.47
40	2.60
50	2,07
60	1.73
65	1.59

Table 3: Evolution of the relative error of the polycentric evaluation of the diffracted field with respect to the distance to Γ, $r_\Gamma = 2\lambda$, $P = 16$.

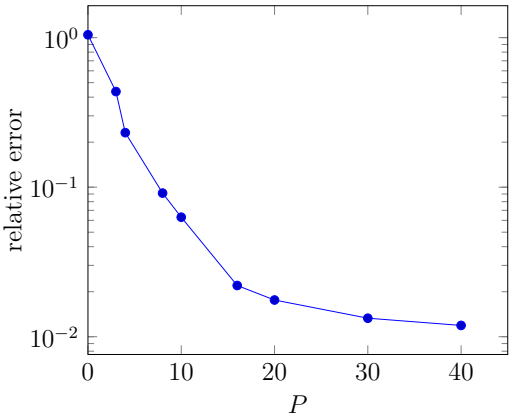

Figure 11: Evolution of the maximum relative error of the diffracted field at 5λ from y_c with respect to the number P of subsets used in the covering of Γ.

the defect is close to a boundary. To conclude, the approach presented is generic and can be extended to 3D elastodynamics, which is our ultimate objective.

References

[1] Watson N G 1966 *A treatize on the theory of Bessel functions* (Cambridge University Press) p194-224
[2] Nedelec J C 2001 *Acoustic and Electromagnetic Equations. Integral representations for harmonic problems* (Applied Mathematical science vol 144) ed Marsden J E and Sirovich L (New-York: Springer-Verlag)
[3] Colton D and Kress R 1998 *Inverse Acoustic Electromagnetic Scattering Theory* (Applied Mathematical Sciences **98**) (Heidelberg: Springer) chapter 3 p37-84
[4] Keller J B and Lewis R M 1995 Asymptotic methods for partial differential equations: the reduced wave equation and the Maxwell's equations, *Surveys in applied mathematics* (Springer US) chapter 1 p1-82
[5] Cerveny G 2000 *Seismic ray theory* (Cambridge University Press)
[6] Runborg O 2007 Mathematical Models and Numerical Methods for High Frequency Waves *Comm. in Comp. Physics* **2** p 827-880
[7] Barbone P R and Michael O 1999 Scattering from submerged objects by a hybrid asymptotic-boundary integral equation method *Wave motion* **29** p137-56
[8] Rokhlin V and Yarvin N 1998 Generalized Gaussian Quadratures and Singular Value Decompositions of Integral Operators *J. on sc. Comp. and Appl. Math.* **20** p699-718